ARTICLE IN PRESS

Simple citric acid-catalyzed surface esterification of cellulose nanocrystals

Jhon Alejandro Ávila Ramírez [a,b], Elena Fortunati [c], José María Kenny [c], Luigi Torre [c], María Laura Foresti [a,b,*]

[a] Grupo De Biotecnología y Biosíntesis, Instituto De Tecnología En Polímeros y Nanotecnología (ITPN), Facultad De Ingeniería, Universidad De Buenos Aires, Las Heras 2214 (CP 1127AAR) Buenos Aires, Argentina
[b] Consejo Nacional De Investigaciones Científicas y Técnicas (CONICET), Argentina
[c] University of Perugia, Civil and Environmental Engineering Department, UdR INSTM, Strada Di Pentima 4, 05100 Terni, Italy

ARTICLE INFO

ABSTRACT

A simple straightforward route for the surface esterification of cellulose nanocrystals (CNC) is herein proposed. CNC obtained from microcrystalline cellulose were acetylated using as catalyst citric acid, a α-hydroxy acid present in citrus fruits and industrially produced by certain molds in sucrose or glucose-containing medium. No additional solvent was added to the system; instead, the acylant (acetic anhydride) was used in sufficient excess to allow CNC dispersion and proper suspension agitation. By tuning the catalyst load, CNC with two different degree of substitution (i.e. DS = 0.18 and 0.34) were obtained. Acetylated cellulose nanocrystals were characterized in terms of chemical structure, crystallinity, morphology, thermal decomposition and dispersion in a non-polar solvent. Results illustrated for the first time the suitability of the protocol proposed for the simple surface acetylation of cellulose nanocrystals.

© 2016 Elsevier Ltd. All rights reserved.

1. Introduction

Cellulose nanocrystals (CNC) obtained by acid treatment of cellulose sources are rigid rod-like particles with a typical acicular structure. CNC are characterized by nanoscaled dimensions that depend on the natural sources or wastes from which they are extracted. The particles are 100% cellulose and highly crystalline, between 54 and 88%. The morphology and the degree of crystallinity of CNC depend on the natural sources used as raw material and the conditions adopted in the extraction process. CNC present important properties as high stiffness, low density (approximately $1.57\,g\,cm^{-3}$), very low thermal expansion coefficient, and high elastic modulus (about 150 GPa). All these interesting characteristics have triggered the use of CNC as reinforcement phase in thermoplastic and/or thermosetting matrices for many different applications (Brinchi, Cotana, Fortunati, & Kenny, 2013; Fortunati et al., 2016; Habibi, Lucia, & Rojas, 2010).

However, the high surface area and hydrophilic nature of cellulose nanocrystals leads to poor dispersibility/compatibility with nonpolar media, resulting in inefficient compounding with most nonpolar polymer matrices in which repulsive forces lead to aggregation and poor interfacial contact. To overcome this problem and broaden the spectrum of polymer matrices in which cellulose nanocrystals can be incorporated, their surface properties need to be transformed to inhibit self-aggregation and improve dispersion and interfacial adhesion, while preserving the original crystalline structure of CNC (Lin, Huang, Chang, Feng, & Yu, 2011). With this aim, in the last years adsorption of amphiphilic surfactants that screen the steric interactions between the cellulose chains, as well as different chemical modification protocols which make use of the abundant hydroxyl groups on the surface of CNC, have been attempted (Eyley & Thielemans, 2014; Habibi, 2014; Heux, Chauve, & Bonini, 2000).

In this context, esterification of CNC has been proposed as a suitable route for conferring hydrophobicity to crystalline cellulose surface and improving their dispersibility/compatibility with hydrophobic polymers when used as a reinforcing phase (Braun & Dorgan, 2009; Fumagalli, Sanchez, Molina Boisseau, & Heux, 2013b; Lin et al., 2011; Wang, Ding, & Cheng, 2007; Yuan, Nishiyama, Wada, & Kuga, 2006). Esterification implies the substitution of hydroxyl groups of cellulose with less polar ester groups. The substitution level is often expressed in terms of the degree of substitution (DS) which is defined as the average number of substituted hydroxyl

* Corresponding author at: Grupo De Biotecnología y Biosíntesis, Instituto De Tecnología En Polímeros y Nanotecnología (ITPN), Facultad De Ingeniería, Universidad De Buenos Aires, Las Heras, 2214 (CP 1127AAR), Buenos Aires, Argentina.
E-mail address: mforesti@fi.uba.ar (M.L. Foresti).

groups per anhydroglucose unit, and has a maximum value of 3. In the last few years, a number of esterification/transesterification methodologies have been applied to hydrophobize CNC, including routes catalysed by sulphuric acid (Tang et al., 2013 (operation at 80 °C during 3–7 h giving a DS of 0.22-0.47); Wang et al., 2007 (40 °C, 3 h, DS = 0.031)), hydrochloric acid (Braun & Dorgan, 2009 (105 °C, 4–25 min, surface DS = 0.25–1.49); Spinella et al., 2015 (150 °C, 3 h, DS = 0.12–0.13)), iodine (Abraham et al., 2016 (110 °C, 0.5 h, DS = 2.1)), potassium carbonate (Cetin et al., 2009 (94 °C, 1 – 24 h, DS = n.a.)), and triethylamine (De Menezes, Siqueira, Curvelo, & Dufresne, 2009 (toluene reflux, 4 h, DS = 0.31 – 0.68)). Esterification reactions in pyridine (Uschanov Johansson, Maunu, & Laine, 2011 (50 °C, 1 h, DS = 0.46–1.20); Zhang, Ma, & Zhang, 2016 (80 °C, 5 h, DS = n.a.)), as well as in the acylant reagent vapour (Berlioz, Molina-Boisseau, Nishiyama, & Heux, 2009 (160–190 °C, 2–13 h, DS = 0.15–1.17); Fumagalli et al., 2013b (150 °C, 2 h, 6 h, DS = 0.07–1.91)), or reagent aqueous emulsion (Yuan et al., 2006 (105 °C, 0.08–2 h, DS ≈ 0.02)), have also been proposed.

In the current contribution, we propose a different straightforward route for the esterification of CNC catalyzed by a naturally-occurring α-hydroxy acid (citric acid) and performed in absence of added solvents. α-Hydroxy acids such as glyceric, glycolic, lactic, malic, mandelic, citric and tartaric acids, are naturally occurring non-toxic biodegradable carboxylic acids which have an hydroxyl group on the carbon adjacent to the carboxyl group. The suitability of certain α-hydroxycarboxylic acids to be used as catalysts in ring-opening polymerizations for the synthesis of polyesters, as well as in the esterification of cellulose fibers has been demonstrated (Hafrén & Córdova, 2005) and recently reviewed (Domínguez de María, 2010). Although their catalytic mechanism has not been completely elucidated, esterifications catalyzed by α-hydroxy acids have been proposed to proceed via a nucleophilic attack of the acylant by the hydroxyl groups of the α-hydroxy acid, followed by second nucleophilic attack of the intermediate formed by the hydroxyl groups of cellulose (Domínguez de María, 2010; Hafrén & Córdova, 2005). In reference to the use of α-hydroxy acids in the esterification of cellulose nanoparticles, some of us have recently reported on the catalytic activity shown by L-tartaric, lactic and citric acids towards the esterification of bacterial cellulose (BC). By using different acylants and reaction conditions, acetylated and propionylated BC samples with DS in the 0.02–0.70 interval could be easily obtained (Ávila Ramírez, Juan Suriano, Cerrutti, & Foresti, 2014; Ávila Ramírez, Gómez Hoyos, Arroyo, Cerrutti, & Foresti, 2016a; Ávila Ramírez, Gómez Hoyos, Arroyo, Cerrutti, & Foresti, 2016b). Based on the previous results on bacterial cellulose esterification, the α-hydroxy acid-catalyzed route is herein extended to the acetylation of cellulose nanocrystals. Despite its potential, to the best of the authors' knowledge, this route has not been applied to CNC hydrophobization before. Characterization of the acetylated CNC including solid state nuclear magnetic resonance spectroscopy (NMR), Fourier transform infrared spectroscopy (FTIR), scanning electron microscopy (SEM), X-ray diffraction (XRD), thermogravimetric analysis (TGA) and dispersibility in apolar liquid medium, is provided.

2. Experimental

2.1. Materials

Microcrystalline cellulose (MCC from wood pulp, dimensions of 10–15 μm) supplied by Sigma Aldrich® was used as precursor to extract nanocrystalline cellulose with nanometric dimensions (CNC). Acetic anhydride (97%, Cicarelli), citric acid (99.5%, Merck), hydrochloric acid (98%, Anedra), sulphuric acid (96%, Sigma Aldrich®), sodium hydroxide (98%, Biopack), potassium hydrogen

phthalate (99.5%, Cicarelli) and sodium carbonate (99%, Mallinckrodt) were all reagent grade chemicals.

2.2. Synthesis of cellulose nanocrystals

Cellulose nanocrystals (CNC) were obtained by a hydrolysis process starting from the commercial MCC (20 g) treated with sulphuric acid (64%wt/wt, 200 mL) at 45 °C for 30 min as reported previously (Cranston & Gray, 2006). Immediately following the acid hydrolysis, the suspension was diluted 20-fold with deionized water to quench the reaction. The obtained suspension was centrifuged at 4500 rpm for 20 min to concentrate the cellulose and to remove excess aqueous acid. The resultant precipitate was dialyzed against water for 5 days by using dialysis tubes, and then an ultrasonic treatment by means of a tip sonicator (Vibracell, 750) for 5 min at 40% of amplitude was performed. The resultant concentration of the aqueous CNC suspension was approximately 0.4% wt/wt. The hydrolysis procedure yield was ca. 20%. The aqueous CNC suspension was then freeze-dried in a Labconco FreeZone 2.5 l Benchtop Freeze Dry System operated at −50 °C and 0.12 mbar during 48 h.

2.3. Chemical modification of CNC

Freeze-dried cellulose nanocrystals (0.7 g dry weight, i.e. 4.32 mmol AGU (anhydroglucose units)) were contacted with acetic anhydride (50 mL, 530 mmol) and citric acid (either 0.26 mmol or 2.6 mmol) in a 100 mL glass flask equipped with a reflux condenser. The mixture was then heated to 120 °C under continuous magnetic agitation in a thermostatized oil bath, and acetylation was run for 3 h. After this period, the solid product was washed in successive centrifugation steps (8500 rpm, 30 min each) first in acetic acid and then in distilled water, to completely remove citric acid and the unreacted acetic anhydride. Finally the aqueous suspension of derivatized CNC was freeze-dried at −50 °C and 0.12 mbar during 48 h.

The level of acetylation conferred to the CNC was determined by heterogeneous saponification and back titration with HCl, as detailed elsewhere (Ávila Ramírez et al., 2014). Briefly, 0.1 g of freeze-dried acetylated CNC were contacted with 20 mL of ethyl alcohol (75%) in 100 mL Erlenmeyer flasks which were heated loosely stoppered during 30 min at 50 °C. Afterwards, the suspensions were brought to slightly basic pH by addition of a 1–2 drops of 0.1 N NaOH using phenolphthalein as indicator. This step assured no contribution of free acid groups (i.e. acid moieties introduced by potential citrate esters) to the measured DS. 20 mL of 0.1N NaOH were then added to each flask, and heated again at 50 °C for 15 min. The flasks were finally allowed to stand tightly stoppered at room temperature for 48 h, after which the excess NaOH was back titrated with 0.1 N HCl, using phenolphthalein as endpoint indicator. A blank determination (neat CNC) was carried through the complete procedure. NaOH and HCl solutions were standardised using previously dried standard potassium hydrogen phthalate and sodium carbonate, respectively. The acyl content and the degree of substitution achieved were then calculated by:

$$Acyl(\%) = [(V_B - V_S) \times N_{HCl} \times 4.3]/W \tag{1}$$

$$DS = (162 \times Acyl\%)/[4300 - (42 \times Acyl\%)] \tag{2}$$

Where V_B (mL) is the volume of HCl required for blank titration, V_S (mL) is the volume of HCl required to titrate the sample, N_{HCl} is the normality of the HCl solution, and W (g) is the mass of sample used.

Free acid functionalities in acetylated CNC which may account for esterified citric acid presence were determined by titration of aqueous suspensions with 0.01 N NaOH using phenolphthalein as end-point indicator.

2.4. Characterization of acetylated CNC

2.4.1. Solid-state CP/MAS ^{13}C NMR spectroscopy (CP/MAS ^{13}C NMR)

High-resolution ^{13}C solid-state spectra of neat and acetylated freeze-dried CNC were recorded using the ramp {1H} → {13C} CP/MAS pulse sequence (cross-polarization and magic angle spinning) with proton decoupling during acquisition. Experiments were performed at room temperature in a Bruker Avance II-300 spectrometer equipped with a 4-mm MAS probe. The operating frequency for protons and carbons was 300.13 and 75.46 MHz, respectively. Glycine was used as an external reference for the ^{13}C spectra and to set the Hartmann-Hahn matching condition in the cross-polarization experiments. The recycling time varied from 5 to 6 s according to the sample. The contact time during CP was 2 ms for all of them. The SPINAL64 sequence (small phase incremental alternation with 64 steps) was used for heteronuclear decoupling during acquisition with a proton field H1H satisfying ω1H/2π = YHH1H = 62 kHz. The spinning rate for all the samples was 10 kHz.

2.4.2. Fourier Transform Infrared Spectroscopy (FTIR)

Fourier transform infrared spectra of neat and acetylated freeze-dried CNC were acquired in transmission mode in an IR Affinity-1 Shimadzu Fourier Transform Infrared Spectrophotometer. Carefully dried (25 mg, 110 °C, 2 h) samples were mixed with previously dried KBr (130 °C, overnight) in the ratio 1:20 and pressed into a disc. Spectra were collected with 40 scans in the 4500–700 cm^{-1} range with a resolution of 4 cm^{-1}, and normalized against the intensity at 1165 cm^{-1} corresponding to the (C—O—C) link of cellulose (Ilharco, García, da Silva, & Ferreira, 1997; Lee et al., 2011).

2.4.3. X-ray diffraction (XRD)

Neat and acetylated freeze-dried CNC were analyzed with a Rigaku D/Max-C Wide Angle automated X-ray diffractometer with vertical goniometer. The X-ray diffraction pattern was recorded in the 10−45° 2θ interval at a step size of 0.02°. Cu/Kα radiation source (0.154 nm), 40 kV, 30 mA were used. Given the high purity of CNC isolated from MCC, the crystallinity index of neat and acetylated CNC samples was estimated from diffraction intensity data by use of Segal's empirical equation (Segal, Creely, Martin, & Conrad, 1959), where I_{002} corresponds to the maximum intensity of the 002 lattice diffraction and accounts for both crystalline and amorphous material, and I_{am} is the intensity at 2θ = 18° and represents amorphous material only.

$$CI = (I_{002} - I_{am})/I_{002} \qquad (3)$$

2.4.4. Scanning Electron Microscopy (SEM)

Drops of diluted aqueous suspensions of neat and acetylated CNC (0.2% w/v) were deposited on microscope glasses, dried at 100 °C for 5 min, coated with gold using an ion sputter coater, and observed by use of a scanning electron microscope Zeiss Supra 40 with Variable Pressure Secondary Electron (VPSE) detector and field emission gun operated at 3 kV. The width of neat and acetylated CNC was determined by using digital image analysis software (ImageJ).

2.4.5. Thermogravimetric analysis (TGA)

Thermogravimetric analysis of neat and acetylated freeze-dried CNC (5.5–6 mg) previously dried at 105 °C during 2 h was conducted in a TGA-50 Shimadzu instrument, in the 25 °C–800 °C interval at a heating rate of 10 °C/min and under nitrogen atmosphere (30 mL/min) in order to prevent thermoxidative degradation. $T_{10\%}$ corresponds to the temperature at which the material weight loss is 10%, whereas T_{max} values correspond to the maximum weight loss rate determined from the first derivative (DTG) of TG signals.

3. Results and discussion

Our previous results have shown the feasibility of acetylating the surface of bacterial cellulose (BC) nanoribbons using as catalysts naturally occurring α-hydroxy acids (e.g. L-tartaric, lactic and citric acids) (Ávila Ramírez et al., 2014, 2016a, 2016b). Particularly, citric acid is the catalyst which showed the highest activity in the acetylation of BC. By proper control of reaction conditions bacterial cellulose nanoribbons with tailored degree of substitution (DS) values within the ≈0.2–0.7 range could be obtained in 3 h of reaction. In the current contribution the citric acid-catalyzed esterification route is extended to the acetylation of cellulose nanocrystals isolated from microcrystalline cellulose. Process conditions (i.e. temperature, acylant volume, reaction time and two catalyst loads) were set based on previous experience aiming to restrict esterification to the surface of CNC. To attain derivatized CNC with two different substitution levels, two catalyst concentrations (i.e. 0.0052 mmol/mL or 0.052 mmol/mL) were used. The corresponding bulk DS values thus obtained as determined by saponification and back titration were 0.18 and 0.34, respectively. Based on previous reports dealing with the esterification of nanocrystalline and nanofibrillated celluloses by this and other methodologies, these DS values seemed appropriate for the goal of achieving surface-only esterification of CNC (e.g. Ávila Ramírez et al., 2014 (BC suspension, acetic acid/propionic acid, tartaric acid as catalyst, 120 °C, 1–8 h, DS = 0.02 − 0.45); Fumagalli, Ouhab, Molina Boisseau, & Heux, 2013a (microfibrillated cellulose aerogels, palmitoyl chloride vapour, 150 °C, 0.5 − 2 h, DS = 0.10 − 0.40); Tang et al., 2013 (CNC, acetic acid, sulfuric acid as catalyst, 80 °C, 3–7 h, DS = 0.22 − 0.47)). By the way, under identical reaction conditions, the DS values herein determined indicated the comparatively lower susceptibility of cellulose nanocrystals to citric acid-catalyzed acetylation with regards to bacterial cellulose (Ávila Ramírez et al., 2016b).

Fig. 1 collects the solid state CP/MAS ^{13}C NMR spectra of native and acetylated CNC. The spectrum of neat CNC displayed the carbon resonances typical for cellulose, assigned to C1 (105.2 ppm), C4 (89.1 ppm), C4′ (84.4 ppm), C2-C3-C5 cluster (68.5-79.7 ppm), C6 (65.3 ppm) and C6′ (62.5 ppm). C4 and C6 resonances are assigned to ordered cellulose structures, whereas the upfield lines C4′ and C6′ are derived from amorphous parts. Compared with neat CNC, acetylated CNC spectra showed new signals characteristic of the groups introduced, confirming the success of the esterification. The signals emerging at 173 and 21 ppm in acetylated CNC spectra are typical of carbons of carbonyl (C=O) and methyl groups (CH$_3$), respectively. The intensity of both increased with the extent of the esterification.

On the other hand, despite the limited resolution of solid state NMR, the absence of resonances at 44 ppm consistent with methylene groups of citric acid, suggests no significant reaction of citric acid itself with the hydroxyl groups of cellulose. This was further confirmed by titration of esterified CNC suspensions with diluted alkali solution, aimed at determining free carboxylic acid functionalities from the potential citrate esters. For the sample contacted with the highest catalyst load used herein (DS = 0.34), titration gave an acid value of 127 ± 9 mmol COOH/kg CNC, which accounts for an esterified citric acid amount of 1.7% of the total citric acid mass introduced (it is assumed that each citrate unit introduces two free carboxylic acids). Under these conditions the contribution of ester citrates to total DS does not exceed 0.01.

FTIR spectra of neat and chemically modified CNC are shown in Fig. 2. Neat CNC presented the typical signals at 1162, 1111, 1060,
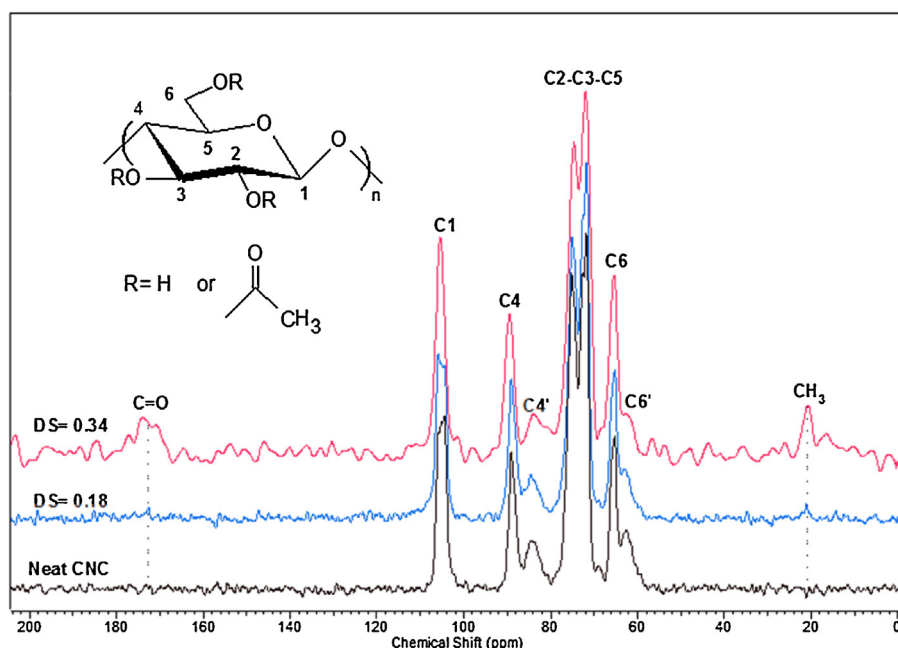
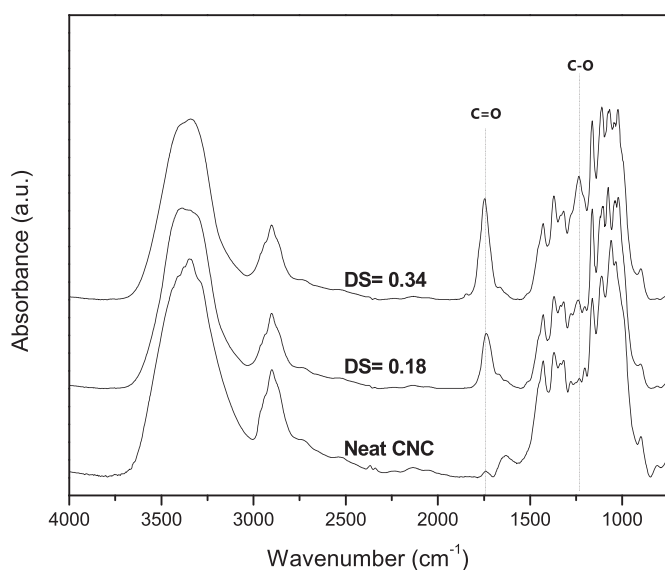**Fig. 1.** Solid state CP/MAS ^{13}C NMR spectra of neat and acetylated CNC.

Fig. 2. FTIR spectra of neat and acetylated CNC.

Fig. 3. Photographs of representative suspensions (1.7 wt%) of freeze-dried samples of (a) neat CNC in water, (b) neat CNC in chloroform, and (c) acetylated CNC with DS = 0.34 in chloroform. Photographs were taken 25 min after sonication at 80W during 3 h.

1030, 895 cm^{-1}, assigned to asymmetric C—O—C bridge stretching, anhydroglucose ring asymmetric stretching, C—O stretching, in-plane C—H deformation and C—H deformation of cellulose, respectively (Nelson & O'Connor, 1964a, 1964b). On the other hand, spectra of chemically treated CNC showed the appearance of signals which gave further proof of acetylation, such as the C=O stretching signal centered at 1737 cm^{-1}, and the C—O stretching vibration observed at 1235 cm^{-1}. Both signals increased with DS.

As a consequence of the partial replacement of hydroxyls by less polar acetyl groups, the high hydrophilicity of CNC is expected to be reduced. Changes in CNC hydrophilicity upon esterification have frequently been characterized by analyzing their dispersibility in different organic solvents and/or their distribution in biphasic polar/non polar liquid systems, as well as by determination of water contact angles (Abraham et al., 2016; Braun & Dorgan, 2009; Cetin
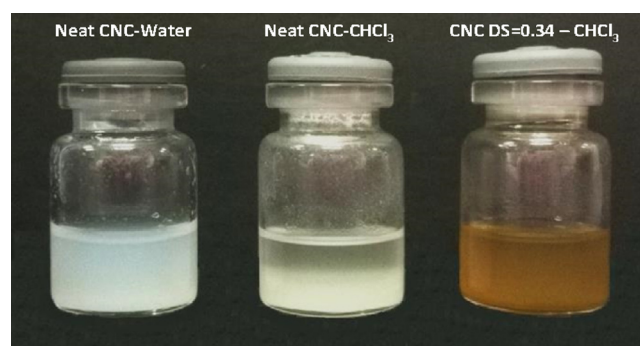
et al., 2009; De Menezes et al., 2009; Fumagalli et al., 2013b; Lin et al., 2011; Wang et al., 2007; Yuan et al., 2006).

Fig. 3 collects photographs of suspensions of neat and acetylated CNC (DS = 0.34) in water and in chloroform. After sonication (3 h, 80W) samples were allowed to stand for 25 min before a photograph was taken. At the concentration tested, resuspended freeze-dried CNC formed a stable suspension in water, whereas neat CNC sedimented quickly in chloroform. On the other hand, the enhanced hydrophobicity conferred to CNC upon acetylation allowed a much better dispersibility of modified CNC (DS = 0.34) in chloroform (Fig. 3). Although settling of modified CNC in chloroform also took place, the effect was significantly less pronounced and slower when compared to neat CNC. The observed behavior encourages the use of the herein esterified CNC as reinforcement of non-polar polymeric matrices, in which alterations of the hydrophilicity of CNC can potentially enhance dispersion and improve nanocomposite properties.

Fig. 4 shows the XRD pattern of neat and derivatized CNC. Neat CNC showed the diffraction features typical of cellulose I crystal domains. The main sharp peak is centred at 2θ = 22.7° (assigned to (002) diffraction plane) that is indicative of the distance between hydrogen bonded sheets in cellulose I domains. The other peaks
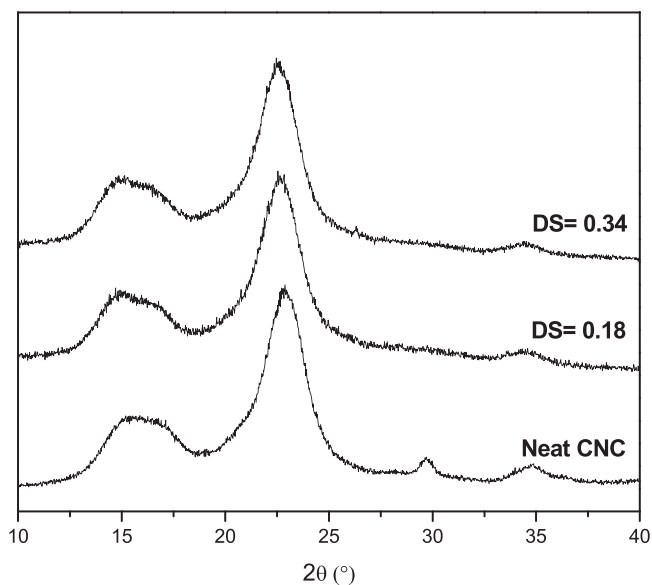
Fig. 4. X- ray diffraction pattern of neat and acetylated CNC.

typical of cellulose I are the herein highly overlapped peaks centred at 15.1° and 16.3° assigned to (101) and (10-1) lattice planes, respectively; and the peak at 34.8° assigned to (040) (Johnson Ford, Mendon, Thames, & Rawlins, 2010; Park, Baker, Himmel, Parilla, & Johnson, 2010). The additional peak at $2\theta = 29.6°$ corresponds to $CaCO_3$ deposits (data confirmed by SEM/EDS analysis) formed upon extensive dialysis of CNC with tap water during their isolation (details in Section 2.2).

The diffraction pattern of neat CNC remained unchanged after citric acid-catalyzed acetylation, suggesting that nanocrystals maintained their original crystalline structure. The crystallinity index of neat and acetylated DS were 0.84 (neat CNC), 0.85 (DS = 0.18) and 0.83 (DS = 0.34); indicating that the esterification occurred mainly at the nanocrystals surface, without affecting their inner crystalline structure. Previous contributions dealing with CNC esterification by other methodologies also observed no sig-

nificant alteration of cellulose I crystallinity for DS values within the 0.02-0.47 interval, which was generally attributed to a surface derivatization process, with most of the crystalline regions being preserved (Tang et al., 2013; Wang et al., 2007; Yuan et al., 2006). Similar conclusions in terms of bulk DS values intervals which restrict modification to cellulose surface have been reported for other nanometric cellulosic substrates (Agustin, Nakatsubo, & Yano, 2016; Ávila Ramírez et al., 2014; Ávila Ramírez et al., 2016a; Ávila Ramírez et al., 2016b; Fumagalli et al., 2013a; Ifuku et al., 2007; Kim, Nishiyama, & Kuga, 2002). The diffraction peak corresponding to $CaCO_3$ deposits ($2\theta = 29.6°$) was no longer observed in the acetylated CNC diffractogram, which is explained by their solubilisation in acetic acid during recovery operations (Section 2.3).

Morphological investigation of neat and derivatized CNC is shown in Fig. 5. FESEM images of neat CNC obtained from the acid hydrolysis procedure showed the typical acicular structure of cellulose nanocrystals with dimensions ranging from 100 to 200 nm in length and $\approx$ 10–20 nm in width. Moreover, CNC appeared well individualized from each other. As shown in Fig. 5, the rodlike shape and also the dimensions of the nanocrystals were not significantly affected by acetylation, suggesting once again that only the surface of the CNC was modified during reaction (Cetin et al., 2009). Surface esterification/transesterification of CNC by other methodologies has frequently been associated with no significant changes in CNC morphology and dimensions. On the other hand, at higher DS values, loss of crystallinity has been often accompanied by the erosion of the CNC structure (Cetin et al., 2009; Lin et al., 2011; Yuan et al., 2006).

Besides crystallinity, another important factor influencing the potential use of CNCs for reinforcement of polymer matrices is their thermostability. The TG and DTG (first derivative of TG data) curves of neat and derivatized CNC are shown in Fig. 6. DTG curves evidence quite close Tmax values for neat and acetylated CNC (i.e. $Tmax_{neatCNC} = 286°C$, $Tmax_{DS=0.18} = 282°C$, $Tmax_{DS=0.34} = 286°C$). However, values for $T_{10\%}$, corresponding to the temperature at which the material weight loss is 10%, illustrate a $\approx 25°C$-reduction upon acetylation ($T_{10\%-CNC} = 254°C$, $T_{10\%-DS=0.18} = 230°C$, $T_{10\%-DS=0.34} = 227°C$). The still relatively high thermal stability of modified CNC suggests their suitability for use in melt-processing operations carried out
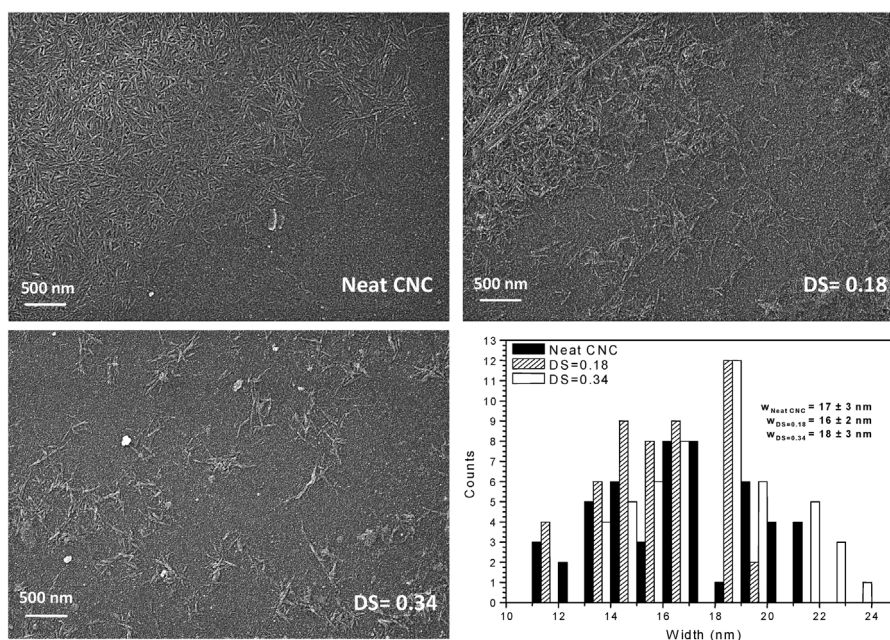

Fig. 5. FESEM images of neat and acetylated CNC and corresponding histogram (width).
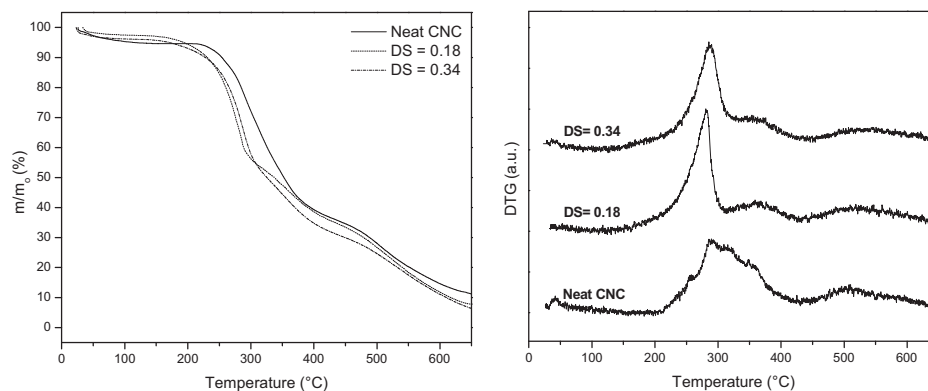
Fig. 6. TG and DTG curves of neat and acetylated CNC.

at moderately high temperatures (Arrieta et al., 2014). Finally, the reduction in the weight loss from room temperature to 130 °C ascribed to water evaporation evidenced the decrease in CNC's hygroscopicity upon acetylation.

4. Conclusions

Cellulose nanocrystals were easily acetylated using citric acid as catalyst, and acetic anhydride as both reagent and reaction medium. The occurrence of the chemical modification was evidenced by new signals characteristic of the ester groups introduced which appeared in the FTIR and NMR ^{13}C spectra of derivatized CNC. Acetate groups covalently attached to the surface of CNC significantly altered their hydrophilicity, as evidenced by their much better dispersibility in chloroform than neat CNC. On the other hand, XRD data indicated that under the conditions chosen, only the surfaces of the nanocrystals were esterified, and the initial crystalline structure of CNC remained unaffected by the chemical treatment.

Given the simplicity and the single-step character of the methodology proposed, as well as the natural origin and non-toxicity of the catalyst used; we conclude that the esterification of cellulose nanocrystals catalyzed by citric acid herein proposed is a promising methodology for surface-only esterification of CNC. To the best of the authors' knowledge, no previous reference to the use of the proposed protocol for the hydrophobization of CNC has previously been reported. Further studies devoted to evaluating the dispersion and reinforcing effect of the produced derivatized CNC in nonpolar polymeric matrices are currently in progress.

Conflict of interest

The authors confirm that this article content has no conflict of interest.

References

Ávila Ramírez, J. A., Juan Suriano, C., Cerrutti, P., & Foresti, M. L. (2014). Surface esterification of cellulose nanofibers by a simple organocatalytic methodology. *Carbohydrate Polymers, 114*, 416–423.

Ávila Ramírez, J. A., Gómez Hoyos, C., Arroyo, S., Cerrutti, P., & Foresti, M. L. (2016a). Naturally occurring α-hydroxy acids: Useful organocatalysts for the acetylation of cellulose nanofibres. *Current Organocatalysis, 3*, 161–168.

Ávila Ramírez, J. A., Gómez Hoyos, C., Arroyo, S., Cerrutti, P., & Foresti, M. L. (2016b). Acetylation of bacterial cellulose catalyzed by citric acid: Use of reaction conditions for tailoring the esterification extent. *Carbohydrate Polymers, 153*, 686–695.

Abraham, E., Nevo, Y., Slattegards, R., Attias, N., Sharon, S., Lapidot, S., et al. (2016). Highly hydrophobic thermally stable liquid crystalline cellulosic nanomaterials. *ACS Sustainable Chemistry & Engineering*, http://dx.doi.org/10.1021/acssuschemeng.5b0136 [in press]

Agustin, M. B., Nakatsubo, F., & Yano, H. (2016). The thermal stability of nanocellulose and its acetates with different degree of polymerization. *Cellulose, 23*, 451–464.

Arrieta, M. P., Fortunati, E., Dominici, F., Rayón, E., López, J., & Kenny, J. M. (2014). Multifunctional PLA-PHB/cellulose nanocrystal films: Processing, structural and thermal properties. *Carbohydrate Polymers, 107*, 16–24.

Berlioz, S., Molina-Boisseau, S., Nishiyama, Y., & Heux, L. (2009). Gas-phase surface esterification of cellulose microfibrils and whiskers. *Biomacromolecules, 10*, 2144–2151.

Braun, B., & Dorgan, J. R. (2009). Single-step method for the isolation and surface functionalization of cellulosic nanowhiskers. *Biomacromolecules, 10*, 334–341.

Brinchi, L., Cotana, F., Fortunati, E., & Kenny, J. M. (2013). Production of nanocrystalline cellulose from lignocellulosic biomass: Technology and applications. *Carbohydrate Polymers, 94*, 154–169.

Cetin, N. D., Tingaut, P., Ozmen, N., Henry, N., Harper, D., Dadmun, M., et al. (2009). Acetylation of cellulose nanowhiskers with vinyl acetate under moderate conditions. *Macromolecular Bioscience, 9*, 997–1003.

Cranston, E. D., & Gray, D. G. (2006). Morphological and optical characterization of polyelectrolyte multilayers incorporating nanocrystalline cellulose. *Biomacromolecules, 7*, 2522–2530.

De Menezes, A. J., Siqueira, G., Curvelo, A. A. S., & Dufresne, A. (2009). Extrusion and characterization of functionalized cellulose whiskers reinforced polyethylene nanocomposites. *Polymer, 50*, 4552–4563.

Domínguez de María, P. (2010). Minimal hydrolases: Organocatalytic ring-opening polymerizations catalyzed by naturally occurring carboxylic acids. *ChemCatChem, 2*, 487–492.

Eyley, S., & Thielemans, W. (2014). Surface modification of cellulose nanocrystals. *Nanoscale, 6*, 7764–7779.

Fortunati, E., Yang, W., Luzi, F., Kenny, J., Torre, L., & Puglia, D. (2016). Lignocellulosic nanostructures as reinforcement in extruded and solvent casted polymeric nanocomposites: An overview. *European Polymer Journal*, http://dx.doi.org/10.1016/j.eurpolymj.2016.04.013 [in press]

Fumagalli, M., Ouhab, D., Molina Boisseau, S., & Heux, L. (2013). Versatile gas-phase reactions for surface to bulk esterification of cellulose microfibrils aerogels. *Biomacromolecules, 14*, 3246–3255.

Fumagalli, M., Sanchez, F., Molina Boisseau, S., & Heux, L. (2013). Gas-phase esterification of cellulose nanocrystal aerogels for colloidal dispersion in apolar solvents. *Soft Matter, 9*, 11309–11317.

Habibi, Y., Lucia, L. A., & Rojas, O. J. (2010). Cellulose nanocrystals: Chemistry, self assembling, and applications. *Chemical Reviews, 110*, 3479–3500.

Habibi, Y. (2014). Key advances in the chemical modification of nanocelluloses. *Chemical Society Reviews, 43*, 1519–1542.

Hafrén, J., & Córdova, A. (2005). Direct organocatalytic polymerization from cellulose fibers. *Macromolecular Rapid Communications, 26*, 82–86.

Heux, L., Chauve, G., & Bonini, C. (2000). Nonflocculating and chiral-nematic self-ordering of cellulose microcrystals suspensions in nonpolar solvents. *Langmuir, 16*, 8210–8212.

Ifuku, S., Nogi, M., Abe, K., Handa, K., Nakatsubo, F., & Yano, H. (2007). Surface modification of bacterial cellulose nanofibers for property enhancement of optically transparent composites: Dependence on acetyl-group DS. *Biomacromolecules, 8*, 1973–1978.

Ilharco, L. M., García, R. R., da Silva, J. L., & Ferreira, L. F. V. (1997). Infrared approach to the study of adsorption on cellulose: Influence of cellulose crystallinity on the adsorption of benzophenone. *Langmuir, 13*, 4126–4132.

Johnson Ford, E. N., Mendon, S. K., Thames, S. F., & Rawlins, J. W. (2010). X-ray diffraction of cotton treated with neutralized vegetable oil-based macromolecular crosslinkers. *Journal of Engineered Fibers and Fabrics, 5*, 10–20.

Kim, D., Nishiyama, Y., & Kuga, S. (2002). Surface acetylation of bacterial cellulose. *Cellulose, 9*, 361–367.

Lee, K.-Y., Quero, F., Blaker, J. J., Hill, C. A. S., Eichhorn, S. J., & Bismarck, A. (2011). Surface only modification of bacterial cellulose nanofibers with organic acids. *Cellulose, 18*, 595–605.

Lin, N., Huang, J., Chang, P. R., Feng, J., & Yu, J. (2011). Surface acetylation of cellulose nanocrystal and its reinforcing function in poly (lactic acid). *Carbohydrate Polymers, 83*, 1834–1842.

Nelson, M. L., & O'Connor, R. T. (1964a). Relation of certain infrared bands to cellulose crystallinity and crystal lattice type. Part I. A new infrared ratio for estimation of crystallinity in celluloses I and II. *Journal of Applied Polymer Science, 8*, 1311–1324.

Nelson, M. L., & O'Connor, R. T. (1964b). Relation of certain infrared bands to cellulose crystallinity and crystal lattice type. Part II. A new infrared ratio for estimation of crystallinity in celluloses I and II. *Journal of Applied Polymer Science, 8*, 1325–1341.

Park, S., Baker, J. O., Himmel, M. E., Parilla, P. A., & Johnson, D. K. (2010). Cellulose crystallinity index: Measurement techniques and their impact on interpreting cellulase performance. *Biotechnology for Biofuels, 3*, 10–20.

Segal, L., Creely, J. J., Martin, A. E., & Conrad, C. M. (1959). An empirical method for estimating the degree of crystallinity of native cellulose using the X-ray diffractometer. *Textile Research Journal, 29*, 786–794.

Spinella, S., Lo Re, G., Liu, B., Dorgan, J., Habibi, Y., Leclére, P., et al. (2015). Polylactide/cellulose nanocrystal nanocomposites: Efficient routes for nanofiber modification and effects of nanofiber chemistry on PLA reinforcement. *Polymer, 65*, 9–17.

Tang, L., Huang, B., Lu, Q., Wang, S., Ou, W., Lin, W., et al. (2013). Ultrasonication-assisted manufacture of cellulose nanocrystals esterified with acetic acid. *Bioresource Technology, 127*, 100–105.

Uschanov, P., Johansson, L.-S., Maunu, S. R., & Laine, J. (2011). Heterogeneous modification of various celluloses with fatty acids. *Cellulose, 18*, 393–404.

Wang, N., Ding, E., & Cheng, R. (2007). Surface modification of cellulose nanocrystals. *Frontiers of Chemical Engineering in China, 1*, 228–232.

Yuan, H., Nishiyama, Y., Wada, M., & Kuga, S. (2006). Surface acylation of cellulose whiskers by drying aqueous emulsion. *Biomacromolecules, 7*, 696–700.

Zhang, X., Ma, P., & Zhang, Y. (2016). Structure and properties of surface-acetylated cellulose nanocrystal/poly(butylene adipate-co-terephthalate) composites. *Polymer Bulletin, 73*, 2073–2085.